Published in final edited form as:
Ann Thorac Surg. 2013 October ; 96(4): 1442–1449. doi:10.1016/j.athoracsur.2013.05.075.

Pulmonary Artery Endothelial Cell Phenotypic Alterations in a Large Animal Model of Pulmonary Arteriovenous Malformations Following the Glenn Shunt

Minoo N. Kavarana, MD[1], **Rupak Mukherjee, PhD**[1], **Shaina R. Eckhouse**[1], **William F. Rawls**[1], **Christina Logdon**[1], **Robert E. Stroud**[1], **Risha K. Patel**[1], **Elizabeth K. Nadeau**[1], **Francis G. Spinale, MD, PhD**[3], **Eric M. Graham, MD**, **Geoffrey A. Forbus**, **Scott M. Bradley, MD**[1], **John S. Ikonomidis, MD, PhD**[1], and **Jeffrey A. Jones, PhD**[1,2]

[1]Division of cardiothoracic Surgery, Medical University of South Carolina, Charleston, SC.

[2]University of South Carolina School of Medicine, Columbia, SC.

[3]Division of Pediatric Cardiology, Medical University of South Carolina, Charleston, SC.

Abstract

Background: Longevity of the superior cavopulmonary connection (SCPC) is limited by the development of pulmonary arteriovenous malformations (PAVM). The goal of this study was to determine whether phenotypic changes in pulmonary artery endothelial cells (PAEC) that favor angiogenesis occur with PAVM formation.

Methods: A superior vena cava to right pulmonary artery connection was constructed in 5 pigs. Pulmonary arteries were harvested at 6-8 weeks following surgery to establish cultures of PAEC and smooth muscle cells, to determine cell proliferation, gene expression, and tubule formation. Abundance of proteins related to angiogenesis was measured in lung tissue.

Results: Contrast echocardiography revealed right-to-left shunting, consistent with PAVM formation. While the proliferation of smooth muscle cells from the right pulmonary artery (RPA) (shunted side) and left pulmonary artery (LPA) (non- shunted side) were similar, right PAEC proliferation was significantly higher. Expression profiles of genes encoding cellular signaling proteins were higher in PAECs from the RPA vs. LPA. Protein abundance of angiopoietin-1, and Tie-2 (angiopoietin receptor) were increased in the right lung (both $p<0.05$). Tubule formation was increased in endothelial cells from the RPA compared to the LPA (404±16 vs. 199±71 tubules/ mm2, respectively $p<0.05$).

Conclusions: These findings demonstrate that PAVMs developed in a clinically relevant animal model of SCPC. This study found that PAVM development occurred concomitantly with differential changes in PAEC proliferative ability and phenotype. Moreover, there was a significant increase in the angiopoietin/Tie-2 complex in the right lung, which may provide novel therapeutic targets to attenuate PAVM formation following a SCPC.

Corresponding Author: Minoo N. Kavarana, MD 96 Jonathan Lucas Street CSB 424/ MSC 613 Charleston, SC 29425-6130 Tel: 843 792 3361 Fax: 843 792 9783 kavarana@musc.edu.

Introduction

The SCPC has been shown to reduce mortality in infants with single ventricle disease before the Fontan procedure.[1] Importantly, some infants who remain palliated by a SCPC fare better than after a Fontan[2] which often demonstrates significant late failures.[3] However, the durability of the SCPC is significantly limited due to progressive cyanosis observed secondary to the development of PAVM's.[4] Therefore, further understanding of factors that contribute to PAVM development may lead to therapies that improve outcomes for these infants.

PAVMs develop due to abnormalities in angiogenesis secondary to changes in blood flow patterns and alterations in the circulating milieu of pro-/anti-angiogenic factors.[5] The SCPC involves directing venous return from the superior vena cava (SVC) to one (classic Glenn shunt) or both (bidirectional SCPC) lungs. This results in a loss of pulsatile flow through the pulmonary arteries (PA), and a change in shear stress and pressure loading conditions on the pulmonary vascular endothelium [6] which may alter the cellular phenotype of pulmonary artery endothelial cells (PAEC).[7] In addition, the redirection of venous return with a SCPC is associated with a loss of hepatic effluent to the lung which has been proposed as a mechanism for PAVM formation after SCPC.[4] Hepatic effluent contains a number of proteins that can promote and/or inhibit angiogenesis.[8] Hepatic stellate cells secrete angiopoietins, which bind to specific receptors on ECs and promote angiogenesis.[9] Conversely, plasminogen, produced by hepatocytes, is the precursor of angiostatin, a potent inhibitor of angiogenesis.[10] However, it remains unknown whether and to what degree these alterations in blood flow patterns and/or loss of hepatic effluent contribute to PAVM development.

Using a porcine model of unidirectional SCPC, we tested the hypothesis that PAVM formation occurs coincident with changes in the phenotypic and functional characteristics of PAECs and/or smooth muscle cells (SMC), with the emergence of a pro-angiogenic signal or the loss of a pre-existing anti-angiogenic signal.

Material and Methods

A unidirectional SCPC was constructed in five pigs (female, 27-31 kg) via a right thoracotomy. The superior vena cava (SVC) and RPA were mobilized and the RPA was temporarily clamped and then completely divided at the bifurcation. The proximal end was sutured close and the distal end anastomosed to the (SVC) using a 10-12 mm Gore-Tex (Gore Medical, Flagstaff, AZ) interposition graft (necessary due to unique porcine PA anatomy). This model results in a lack of pulsatile flow to the RPA and antegrade pulsatile flow to the LPA. The left lung and LPA served as contralateral controls for the right lung and RPA. The lungs and PA's from two age-matched pigs were harvested and used as referent control specimens, which were used to account for changes in unknown circulating factors that could influence the phenotype of PAECs from the LPA. Hemodynamic measurements including oxygen saturation was measured at baseline and during the terminal procedure. Animals were treated and cared for in accordance with the National Institutes of Health "Guide for the Care and Use of Laboratory Animals" (National Research Council, Washington, 1996), and the Institutional Animal Care and Use Committee approved the protocol.

At 6-8 weeks following SCPC, contrast echocardiography and angiography were performed to ascertain PAVM formation. Right and left lung biopsies were obtained at each terminal experiment (n=7, 5 pigs with a SCPC and 2 referent controls), and stored in formalin for immunohistochemistry or flash frozen.

PAECs and SMCs were isolated from the right (RPA/SCPC side; n=2 PAEC, n=3 SMC) and left (LPA/non-shunted side; n=3 PAEC, n=3 SMC) PA from the SCPC pigs. In addition, PAECs and SMC cells were isolated from the RPA; (n=2 PAEC, n=2 SMC) and LPA; (n=2 PAEC, n=2 SMC) from the referent controls. Each cell line was assayed in triplicate and values for each pig were averaged to form a single data point.[11] Briefly, the PA's were opened and the luminal surface scraped into porcine EC growth media (Cell Applications, San Diego, CA). SMCs from the PA's were cultured using the outgrowth technique[12]. The PA's were minced into 2mm × 2mm pieces and cultured in Smooth Muscle Growth Media 2; (Promocell, Heidelberg, Germany) containing 20% FBS (Life Technologies, Grand Island, NY). The cells were incubated at 37°C, 5% CO_2 (21% O_2) and allowed to propagate until time of studies. All cell cultures were analyzed in early passages three through eight.

Cell Proliferation Assay

Cell proliferation was quantified utilizing the CyQuant Assay (Life Technologies). PAEC and SMCs were seeded in a 96 well plate (Corning Inc., Corning, NY) at a density of 5×10^3 cells per well. Cells were then stained with 0.004% CyQuant Direct nucleic stain in PBS and a direct background suppressor (0.02%) for 1 hour at 37°C with 5%CO_2. Fluorescence (excitation/emission: 480/535 nm), which reflected the number of cells, was measured at standard time-points of 24, 30, 44, 54, and 68 hours following seeding and expressed as a change in cell number from the 24 hour time point [13].

Tubule Formation Assay

Tubule formation assay was performed to determine a functional phenotype for the EC.[11] PAECs (1.2×10^5 cells /well) were added to 24-well plates coated with basement membrane matrix (298 μL, Matrigel, 9.2mg/ml per well; BD Biosciences, San Jose CA). Cells were incubated at 37°C for 3 hours and imaged (2.5× objective; Zeiss Axiovert, Germany). Number of tubules, length of the tubules, and nodes at which the tubules originated were identified using a tracking algorithm and quantified by image analysis (SigmaScan Pro 5, Systat Software, San Jose, CA).

Quantitative Polymerase Chain Reaction (QPCR)

PAECs from the LPA and RPA from SCPC animals and controls were denatured to extract RNA, which was reverse transcribed to generate cDNA (RT^2 First Strand Kit, Qiagen). cDNA was stored at −80°C until analyzed by quantitative PCR. Each cDNA sample was loaded onto a custom designed PCR Array (Qiagen). The list of primers and gene sequences are provided in Appendix Table 1 (an Appendix for this article is available in the Auxiliary Annals section of the STS website: http://www.sts.org/auxiliaryannals/Kavarana-2013-Vol-Issue-Page-Appendix.pdf). Each sample was amplified (CFX96, Bio-Rad Hercules, CA) with gene specific primer/probe sets to determine the cycle threshold (C_t) value for the gene of interest. Negative controls were run to verify the absence of DNA contamination. The mean Ct value for two control genes, HPRT1 and GAPDH, were used to normalize the data and calculate relative expression levels using the ΔCt method.[14] The relative expression levels were calculated as a fold change from the control using the ΔΔCt method. Fold changes greater than 2-fold and less than 0.5 fold were marked as statistically different. Genes were categorized as those related to extra-cellular matrix (ECM) degradation, ECM deposition, and cellular signaling. The sum of fold changes in the expression of genes in each category was computed and plotted on a 3-axis matrix (radar plot) as previously described.[14]

Immunoblotting

Immunoblotting was performed on lung homogenates and PAEC cell lysates.[15] Lung tissue extracts and PAEC cell lysate (20 μg total protein) were subjected to electrophoretic separation and transferred to a nitrocellulose membrane. Following blocking and washing, membranes were incubated for 1 hour in anti-sera corresponding to the specific analyte of interest (Appendix Table 2, an Appendix for this article is available in the Auxiliary Annals section of the STS website: http://www.sts.org/auxiliaryannals/Kavarana-2013-Vol-Issue-Page-Appendix.pdf). Relative abundance of each analyte was analyzed by scanning densitometric methods using Gel-Pro Analyzer (Media Cybernetics Inc., Silver Spring, MD) and normalized to β-actin values.

Statistical analysis

For each analysis, the normality of data distribution across all groups was analyzed using the Shapiro-Wilk test. Data for any analyte not normally distributed was transformed prior to making statistical comparisons. Data points were expressed as a mean ± standard deviation, and groups were compared using parametric statistics. Immunoblotting results were expressed as a percent change from referent control values (set to 100%). Comparisons were performed using a two-sided, one sample t-test. Changes in SMC and PAEC proliferation, and PAEC tube formation, were examined using a one-way ANOVA. Because control RPA and LPA groups demonstrated no significant inter-group differences in proliferation, tube formation, or gene expression, control RPA and LPA results were combined to represent a single referent control group. Statistical procedures were performed using either BMDP (Cork, Ireland) or STATA (Statacorp, College Station, TX) software packages. Values of $P<0.05$ were considered statistically significant.

Results

At 6–8 weeks following creation of a SCPC, contrast echocardiography (Figure 1A) showed significant right-to-left shunting consistent with PAVM formation. [16] Pulmonary angiography demonstrated PAVMs in the right lung. There were no significant differences in oxygen saturations between controls and SCPC animals (98.0±0.3% vs. 91.6±4.9%, p=0.23).

In lung homogenates (Figure 1B), protein abundance of angiopoietin-1 and angiostatin, were higher in the RPA group when compared to LPA and controls. However, abundance of Tie-2, vascular endothelial growth factor (VEGF), endoglin, and KLF-2 (shear-stress responsive transcription factor) were similar between groups. In addition, hypoxia-responsive factors, hypoxia-induced factor (HIF-1α) and heme-oxygenase (HO-1), were found to be similar between groups.

To examine the contribution of changes in cellular function toward PAVM development, RPA and LPA PAECs and SMCs were isolated and multiple primary cell lines were established from SCPC and controls. Key hallmarks of cellular phenotype were examined including, proliferation, protein abundance, gene expression, and tube formation.

Cell Proliferation Assay

While the number of SMCs increased over time in each group of cell lines, no difference in growth rate was observed (Figure 2A). The number and growth rate of PAECs in the RPA, however, increased significantly, as compared to the LPA and controls (Figure 2B); RPA (17.9±12.9; $p<0.05$) vs. LPA (3.2±2.0) or referent control (3.7±0.7), expressed as percent change in cell number/hr. The RPA ECs were more prolific and there were a larger number of cells when plates were examined at similar times after plating (Figure 2C). However, ECs

from the LPA, and RPA at the same confluence (similar number of cells) were morphologically similar (Figure 2D).

Immunoblotting and QPCR

Protein abundance of endoglin, KLF2, and Tie-2, were examined in each group of PAECs (Figure 3A-D). Abundance of endoglin (Figure 3B) and Tie-2 levels (Figure 3D) were increased in the RPA group when compared to the LPA and controls. However, abundance of KLF-2 was similar between all groups. When comparing expression profiles of genes involved in ECM deposition, ECM degradation, and cellular signaling, multiple genes displayed a differential pattern of expression in the ECs isolated from the RPA versus the LPA and control groups (Table 2, online supplement). When expressed as a radar plot (Figure 4), the gene expression profile for the RPA was clearly different than that of the LPA group and control group, with a relative increase in the genes related to cellular signaling.

Tubule Formation

Photomicrographs from 3 hour tubule-formation assays are shown (Figure 5A). There was a greater number of tubules formed by cells from the RPA vs. the LPA and control within 3 hours of seeding. The number (Figure 5B) and total length of tubules (Figure 5C) were higher in the RPA group vs. LPA and controls ($p<0.05$). However, the average lengths of cells were not different between the groups (28±1 vs. 26±1 μm). This demonstrated a greater angiogenic potential in the RPA group.

Comment

SCPC creation results in a loss of pulsatile blood flow and hepatic effluent.[4,6] Both these factors can affect function and paracrine signaling in PAECs via modulation of angiogenesis.[7,17] Changes in EC function have previously been associated with AVMs in the brain.[11] Contrast echocardiography in infants following SCPC has demonstrated right-to-left shunting through PAVM formation almost universally.[18] Consistent with this, creation of a SCPC in our study resulted in PAVMs. Concomitantly RPA PAECs exhibited a phenotypic change with higher proliferation rates, increased abundance of angiogenic factors, and stable alterations in gene expression profile that translate into a faster rate of tubule formation as compared to the LPA or controls. Thus, for the first time, this study demonstrated that changes in PAEC phenotype are associated with PAVM formation induced by the SCPC, and identifies mediators that may provide novel targets to attenuate PAVM development.

Non-pulsatile flow following a SCPC has been implicated in PAVM development.[6] Alterations in shear stress and pressure loading conditions can alter EC phenotype.[7] In order to examine the contribution of shear stress in PAVM development, KLF-2 abundance was examined. [19] Levels were similar in lung tissue and isolated PAECs in the presence and absence PAVMs. This suggests that flow related changes did not contribute to PAVM development. However we did not assess the effect of shear stress on SMC phenotype.

The rationale for using a porcine model was based on the similarities to the human cardiovascular system.[20] Previous studies have demonstrated PAVM development following a SCPC using other species.[8,17] Following SCPC creation in lambs increased angiotensin II expression in lungs with PAVMs was observed. [8] Gene array analysis of lung homogenates in a rat model has previously demonstrated altered expression of angiogenic factors.[17] However, changes reported from both models were analyzed from lung tissue homogenates,

which consist of diverse cell types. We measured the relative protein abundance of specific analytes in lung homogenates to examine changes between SCPC lungs and controls.

In order to more closely examine the role of the specific cell types involved in the aberrant angiogenesis leading to PAVMs, we isolated and cultured primary PAECs and SMCs. When we examined protein analytes in isolated cultures we found increased levels of Tie-2 and endoglin (Fig 1B), both endothelial specific markers, which were enriched by isolated cell cultures. Finding differential abundance of endoglin and Tie-2 in RPA versus LPA and controls provided significant evidence that the RPA PAEC phenotype was altered following the SCPC.

A role for altered oxidative stress in the development of PAVMs has been suggested.[21] Three groups were compared in an ovine model: SCPC, PA banding, and sham surgery with 30 minutes of RPA occlusion. The SCPC and PA banded cohorts had an increase in expression of oxidative stress genes; HIF-1 and HO-1 over the sham cohort. This suggested that PAVMs may result from hypoxia and increased oxidative stress. In our study, there were no differences in gene expression of these markers. HIF-1 is known to be induced by hypoxia or ischemia.[22] While in single ventricle patients this is indeed the case, the SCPC model is created in the setting of normal cellular and tissue oxygenation. Therefore the lack of significant hypoxia does not support oxidative stress as an etiologic mechanism of PAVM formation.

Convincing clinical evidence of the liver's role in PAVM development comes from heterotaxy patients who after a SCPC have hepatic venous blood diverted away from both lungs, and develop bilateral PAVMs.[4] Interestingly, these patients demonstrate dramatic resolution of PAVMs with redirection of hepatic venous return to the lungs.[4] Similarly, patients with end stage liver disease develop PAVMs which resolve following liver transplant.[23] These findings suggest that PAVM development is associated with the absence of anti-angiogenic factors or an increase in factors that promote angiogenesis in lungs with PAVMs. Pro-angiogenic factors include angiopoietin-1/Tie-2 complex and VEGF/VEGF receptor complex, while anti-angiogenic factors angiostatin and endostatin, inhibit angiogenesis. A recent study observed decreased endostatin levels in patients with a SCPC.[24] Our study demonstrated that the expression of angiopoietin-1 was increased in lung homogenates from SCPC pigs as compared with controls. We examined endostatin abundance in lung homogenates and were unable to consistently detect a signal on immunoblots at the appropriate molecular weights. Together with the findings of PAEC proliferation and tubule forming capacity, these results demonstrate that PAVM formation is associated with an elevation of factors that promote angiogenesis.

Isolated ECs from human brain AVMs overexpress proangiogenic factors and proliferate faster than ECs in brains without AVMs.[11] Similarly, in our study PAECs from lungs with PAVMs demonstrated a significantly higher proliferation rate than controls. Moreover, results from the tubule formation assay provided functional evidence of increased angiogenic potential in RPA ECs. The determination of a PAEC phenotype with respect to proliferation can provide a valuable *in vitro* test bed to determine fundamental mechanisms for PAVM development.

Hereditary hemorrhagic telangiectasia (HHT) is an autosomal disorder characterized by multisystem vascular dysplasias with a high incidence of PAVMs.[25] Mutations in endoglin, a receptor that binds transforming growth factor (TGF)-β, have been identified with increased angiogenesis.[25] We found increased endoglin levels in the right lung. Gene expression profiles of the RPA PAEC demonstrated an increased expression of genes related to cellular signaling. Since, the effect of selective inhibition of the TGF-β receptor has

demonstrated inhibition of tumor proliferation and angiogenesis,[26] manipulation of this pathway may provide a means to attenuate pathological angiogenesis and PAVM formation.

Limitations and conclusions

While the LPA control within the SCPC animal accounts for lack of IVC effluent in the RPA, the control animals account for non-pulsatile flow in the SCPC. We did not exclusively account for the potential effects of temporary clamping during surgery. Changes in protein levels and PAEC phenotype were examined after PAVM formation, which therefore precluded the examination of fundamental processes that contribute to the initiation and progression of PAVMs. Follow up studies will incorporate controls and time points accounting for these variables.

A potential limitation of this study is that it was performed in a relatively small group of animals. Further, the SCPC was created in physiological normal animals, which may not be an accurate reproduction of the human condition. Therefore, findings from this study would need to be validated in humans.

In conclusion, our findings suggest that PAVM formation following SCPC in pigs was associated with phenotypic changes in PAECs from the RPA. While this study does not confirm the role of a hepatic factor, these alterations in PAEC proliferation rate, protein abundance, gene expression, and tubule formation play a mechanistic role in the development of PAVMs. Persistent changes in gene expression may provide novel therapeutic targets in the management of children with PAVMs following SCPC palliation. These results suggest that PAVM development is enhanced through the promotion of angiogenesis via the Angiopoietin-1/Tie 2 pathway.

Supplementary Material

Refer to Web version on PubMed Central for supplementary material.

Acknowledgments

We acknowledge the contribution by Mrs. Martha Stroud, a biostatistician, in reviewing the statistical methods employed for this study.

This study was supported by NIH grants HL089170 (JSI), HL057952, HL059165. HL095608 (FGS), T32 HL007260 (SRE), and Merit Awards from the Veterans' Affairs Health Administration (FGS, JAJ).

Abbreviations and Acronyms

AVM	arteriovenous malformations
EC	endothelial cell
ECM	extracellular matrix
HHT	Hereditary hemorrhagic telangiectasia
HIF-1	Hypoxia inducible factor-1
HO-1	Hemoxygenase -1
LPA	left pulmonary artery
PAEC	pulmonary artery endothelial cell
PAVM	pulmonary arteriovenous malformation

RPA	right pulmonary artery
SCPC	superior cavopulmonary connection
SMC	smooth muscle cell
SVC	superior vena cava
TGF- β	transforming growth factor- β
VEGF	Vascular endothelial growth factor

References

1. Jonas RA. Indications and timing for the bidirectional Glenn shunt versus the fenestrated Fontan circulation. The Journal of thoracic and cardiovascular surgery. 1994; 108:522–4. [PubMed: 7521499]
2. Day RW, Etheridge SP, Veasy LG, et al. Single ventricle palliation: greater risk of complications with the Fontan procedure than with the bidirectional Glenn procedure alone. Int J Cardiol. 2006; 106:201–10.
3. Fontan F, Kirklin JW, Fernandez G, et al. Outcome after a "perfect" Fontan operation. Circulation. 1990; 81:1520–36.
4. McElhinney DB, Kreutzer J, Lang P, Mayer JE Jr. del Nido PJ, Lock JE. Incorporation of the hepatic veins into the cavopulmonary circulation in patients with heterotaxy and pulmonary arteriovenous malformations after a Kawashima procedure. The Annals of thoracic surgery. 2005; 80:1597–603. [PubMed: 16242423]
5. Starnes SL, Duncan BW, Kneebone JM, et al. Angiogenic proteins in the lungs of children after cavopulmonary anastomosis. The Journal of thoracic and cardiovascular surgery. 2001; 122:518–23. [PubMed: 11547304]
6. Marianeschi SM, McElhinney DB, Reddy VM. Pulmonary arteriovenous malformations in and out of the setting of congenital heart disease. Ann Thorac Surg. 1998; 66:688–91. [PubMed: 9725455]
7. Brooks AR, Lelkes PI, Rubanyi GM. Gene expression profiling of human aortic endothelial cells exposed to disturbed flow and steady laminar flow. Physiological genomics. 2002; 9:27–41.
8. Malhotra SP, Reddy VM, Thelitz S, et al. Cavopulmonary anastomosis induces pulmonary expression of the angiotensin II receptor family. The Journal of thoracic and cardiovascular surgery. 2002; 123:655–60. [PubMed: 11986592]
9. Asahara T, Chen D, Takahashi T, et al. Tie2 receptor ligands, angiopoietin-1 and angiopoietin-2, modulate VEGF-induced postnatal neovascularization. Circulation research. 1998; 83:233–40. [PubMed: 9710115]
10. Clement B, Musso O, Lietard J, Theret N. Homeostatic control of angiogenesis: A newly identified function of the liver? Hepatology. 1999; 29:621–3.
11. Jabbour MN, Elder JB, Samuelson CG, et al. Aberrant angiogenic characteristics of human brain arteriovenous malformation endothelial cells. Neurosurgery. 2009; 64:139–46. discussion 46-8. [PubMed: 19145162]
12. Li XH, Peng J, Tan N, et al. Involvement of asymmetric dimethylarginine and Rho kinase in the vascular remodeling in monocrotaline-induced pulmonary hypertension. Vascular pharmacology. 2010; 53:223–9. [PubMed: 20840872]
13. Jones LJ, Gray M, Yue ST, Haugland RP, Singer VL. Sensitive determination of cell number using the CyQUANT cell proliferation assay. Journal of immunological methods. 2001; 254:85–98.
14. Jones JA, Beck C, Barbour JR, et al. Alterations in aortic cellular constituents during thoracic aortic aneurysm development: myofibroblast-mediated vascular remodeling. Am J Pathol. 2009; 175:1746–56. [PubMed: 19729479]
15. Wilson EM, Moainie SL, Baskin JM, et al. Region- and type-specific induction of matrix metalloproteinases in post-myocardial infarction remodeling. Circulation. 2003; 107:2857–63. [PubMed: 12771000]

16. Chang RK, Alejos JC, Atkinson D, et al. Bubble contrast echocardiography in detecting pulmonary arteriovenous shunting in children with univentricular heart after cavopulmonary anastomosis. J Am Coll Cardiol. 1999; 33:2052–8. [PubMed: 10362213]

17. Tipps RS, Mumtaz M, Leahy P, Duncan BW. Gene array analysis of a rat model of pulmonary arteriovenous malformations after superior cavopulmonary anastomosis. The Journal of thoracic and cardiovascular surgery. 2008; 136:283–9. [PubMed: 18692629]

18. Vettukattil JJ, Slavik Z, Lamb RK, et al. Intrapulmonary arteriovenous shunting may be a universal phenomenon in patients with the superior cavopulmonary anastomosis: a radionuclide study. Heart. 2000; 83:425–8.

19. Dekker RJ, van Soest S, Fontijn RD, et al. Prolonged fluid shear stress induces a distinct set of endothelial cell genes, most specifically lung Kruppel-like factor (KLF2). Blood. 2002; 100:1689–98. [PubMed: 12176889]

20. Rodrigues M, Silva AC, Aguas AP, Grande NR. The coronary circulation of the pig heart: Comparison with the human heart. Eur J Anat. 2005; 9:67–87.

21. Malhotra SP, Reddy VM, Thelitz S, et al. The role of oxidative stress in the development of pulmonary arteriovenous malformations after cavopulmonary anastomosis. The Journal of thoracic and cardiovascular surgery. 2002; 124:479–85.

22. Semenza GL. HIF-1 and human disease: one highly involved factor. Genes & development. 2000; 14:1983–91.

23. Laberge JM, Brandt ML, Lebecque P, et al. Reversal of cirrhosis-related pulmonary shunting in two children by orthotopic liver transplantation. Transplantation. 1992; 53:1135–8. [PubMed: 1585477]

24. Field-Ridley A, Heljasvaara R, Pihlajaniemi T, et al. Endostatin, an inhibitor of angiogenesis, decreases after bidirectional superior cavopulmonary anastamosis. Pediatric cardiology. 2013; 34:291–5.

25. McAllister KA, Grogg KM, Johnson DW, et al. Endoglin, a TGF-beta binding protein of endothelial cells, is the gene for hereditary haemorrhagic telangiectasia type 1. Nature genetics. 1994; 8:345–51. [PubMed: 7894484]

26. Wan X, Li ZG, Yingling JM, et al. Effect of transforming growth factor beta (TGF-beta) receptor I kinase inhibitor on prostate cancer bone growth. Bone. 2011

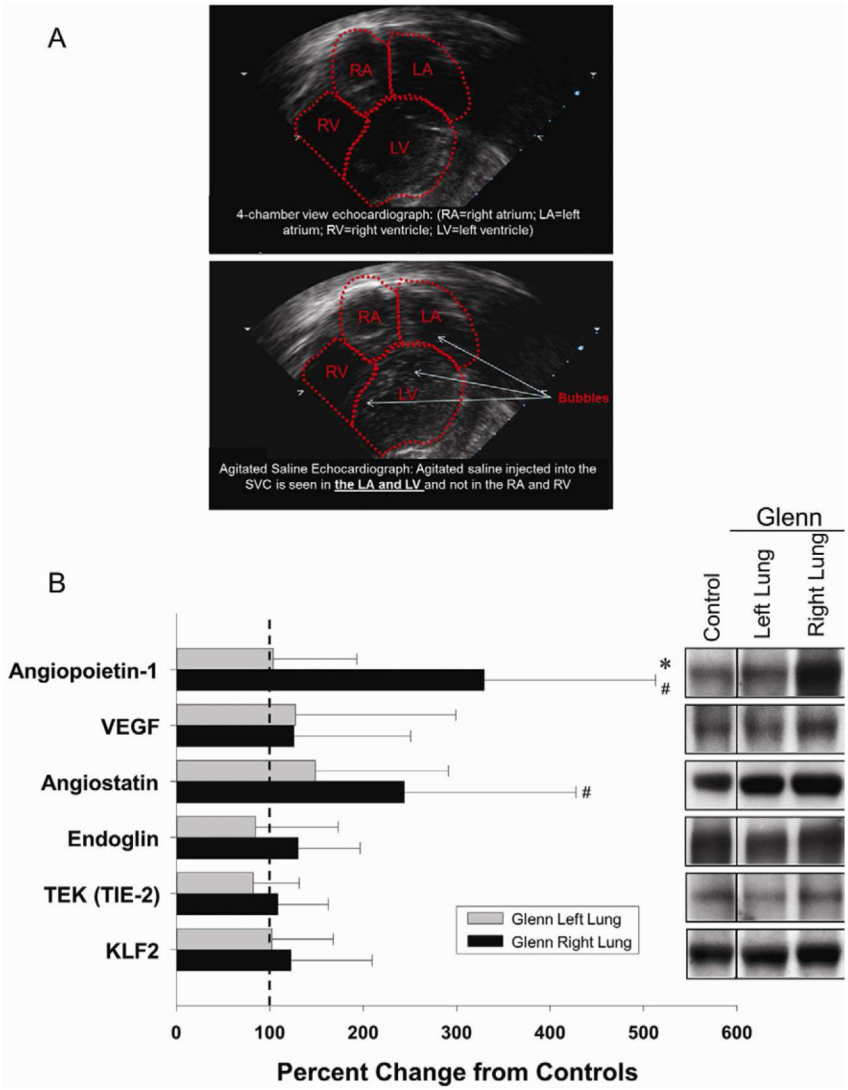

Figure 1.

A. 2-D contrast echocardiogram showing PAVMs. **B.** Protein abundance of angiopoietin-1, angiostatin, Tie-2, endoglin, KLF-2, and VEGF in the right lung of SCPC pigs expressed as a fold change from values obtained in the left lung of the SCPC pigs and controls (set to 100%; dashed vertical line). *p<0.05 vs. right lung, # left lung SCPC.

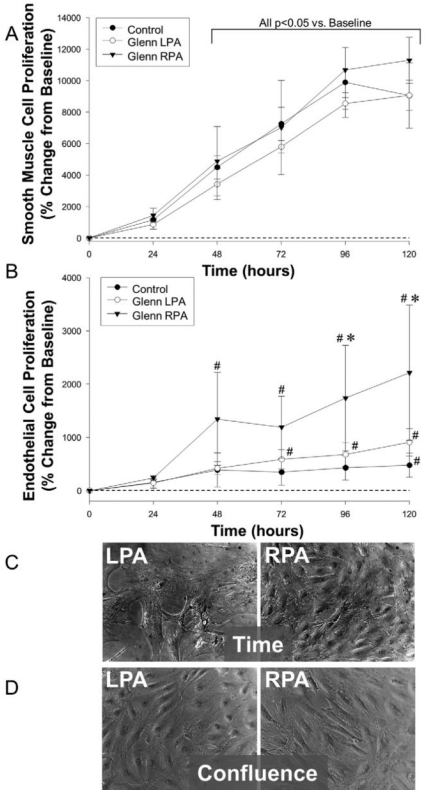

Figure 2.

A. Proliferation of SMCs from the LPA, RPA and controls expressed as a change from the 24 hour time point (set to zero). There were no differences between the LPA and the RPA (# $p<0.05$ vs. “time 0”).

B. Proliferation of RPA ECs was higher than the LPA and controls (*$p<0.05$ vs. LPA; # $p<0.05$ vs. “time 0”).

C. Photomicrographs of ECs from the LPA and RPA at similar confluence.

D. Photomicrographs of ECs from the LPA and RPA pig at 5 days after plating.

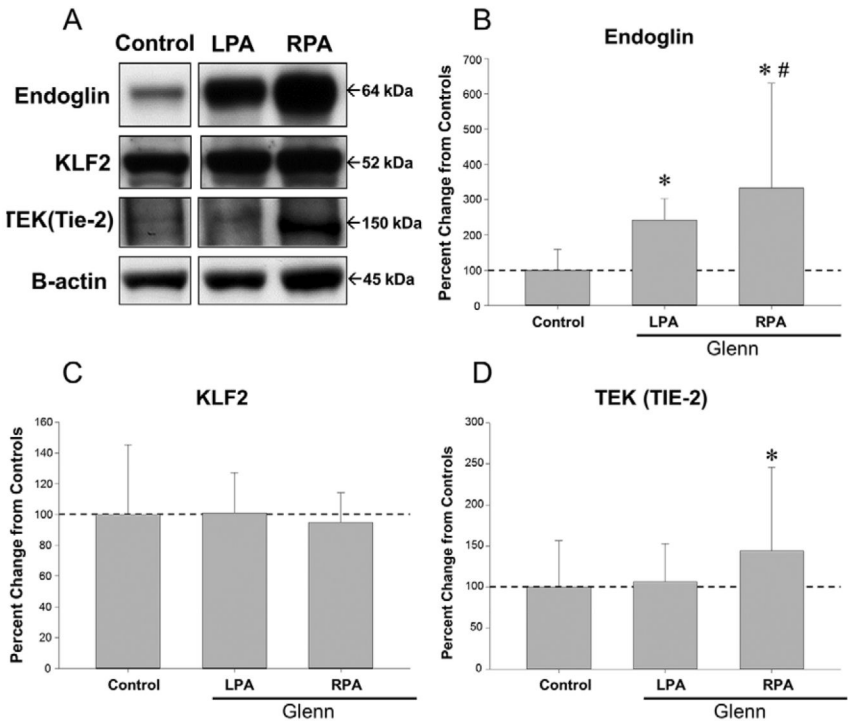

Figure 3.

A. Immunoblots for endoglin, KLF-2, Tie-2, and β-actin in lysates of ECs from the LPA, RPA and control. KLF-2 (**C**) abundance was statistically similar between LPA, RPA and controls; endoglin (**B**) and Tie-2 abundance (**D**) was higher in the RPA than in the LPA. (*$p<0.05$ vs. LPA).

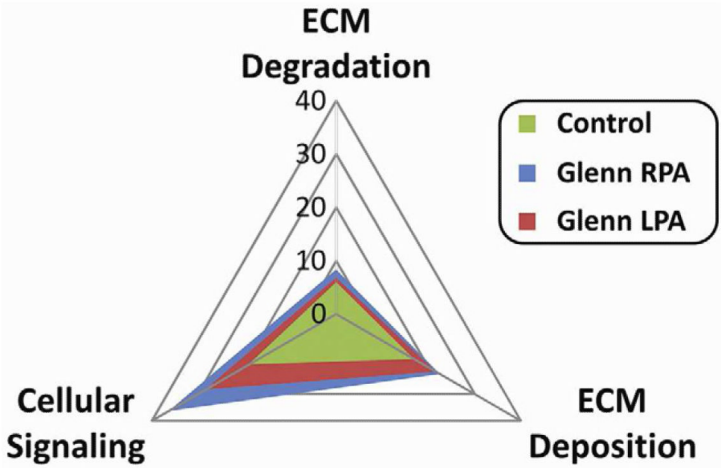

Figure 4.

Radar plot showing relative gene expression profiles for genes related to ECM degradation, ECM deposition, and cellular signaling. The plot for the LPA (plane defined by the red triangle) and control (plane defined by the green triangle) was clearly different than the plane defined for the RPA (blue triangle). Fold expression levels for the genes that resulted in this plot are summarized in Appendix Table 1.

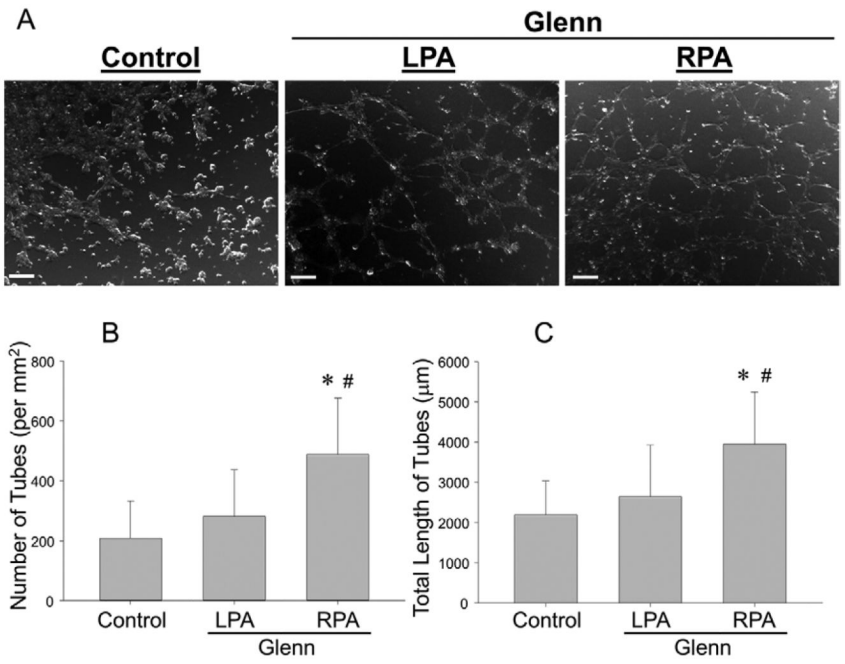

Figure 5.

A. Photomicrographs of ECs from the LPA, RPA and controls 3 hours after plating. Cells from the LPA (left) and controls assembled into a number of nodes and tubule extension had commenced as evidenced by thin structures between nodes. In contrast, cells from the RPA – at the same time point – had assembled into a well-defined network structure between nodes, consistent with a more pro-angiogenic phenotype. Number of tubes (**B**) and total length of tubes (**C**) were higher in the RPA than in the LPA (*$p<0.05$ vs. LPA).